Zeitschrift: IABSE reports of the working commissions = Rapports des commissions de travail AIPC = IVBH Berichte der Arbeitskommissionen

Band: 11 (1971)

Artikel: Research works on ultimate strength of plate girders and Japanese provisions on plate girder design

Autor: Fujii, Tokio / Fukumoto, Yuhshi / Nishino, Fumio

DOI: https://doi.org/10.5169/seals-12051

Research Works on Ultimate Strength of Plate Girders and Japanese Provisions on Plate Girder Design

Recherches sur la résistance à la ruine des poutres à âme pleine et Règles Japonaises concernant les poutres à âme pleine

Forschungsbeiträge zur Tragfähigkeit von Blechträgern und Japanische Vorschriften über Blechträger

TOKIO FUJII
Dr. Chief Research Engineer, Research Inst.
Ishikawajima-Harima Heavy Industries Co., Ltd. Japan

YUHSHI FUKUMOTO
Ph.D. Associate Professor
Nagoya University, Japan

FUMIO NISHINO
Ph.D. Associate Professor
University of Tokyo, Japan

TOSHIE OKUMURA
Dr. Professor
University of Tokyo, Japan

1. INTRODUCTION

Plate Girder Committee at the Society of Steel Construction of Japan (JSSC) has been working on the general investigation of the behavior of the welded plate girder under static and dynamic loads. The purpose of the investigation was primarily to review the experimental studies which had been conducted in various countries and the results were summarized in JSSC Journals (in Japanese) Vol. 4, No. 27, 1968, pp. 1-73. The design practices of plate girders in bridges, buildings and ship structures and the current provisions of the plate girder design were also included in the volume.

In the first part of this report, the research works on the ultimate strength of plate girders which have been carried out by the authors, the Committee members of JSSC, are described independently. That is,

2.1 Ultimate Strength of Plate Girders by T. Fujii,
2.2 Lateral Collapse of Plate Girders in Bending by Y. Fukumoto, and
2.3 Load-Deformation Characteristics of Plate Girders by F. Nishino and T. Okumura.

In the second part, the current Japanese specifications for the plate girder design in railway and highway bridges, buildings and ship structures are reviewed briefly.

2. RESEARCH WORKS

2.1 Bending and Shear Strength of Plate Girders

(1) Shear Strength of Plate Girders

Fujii has introduced the theoretical formulas for calculating the ultimate shear strength of plate girder webs including the effect of the stiffness of flange plate[1][2] The results are summarized in Table 2.1.1.

Table 2.1.1 Summary of Ultimate Shear Strength of Plate Girders

Failure Mode	Requisite Condition	Ultimate Shear Force	
 $\lvert\sigma_1-\sigma_2\rvert=\sigma_{wY}$ $\sigma_2=-\tau_{cr}\sin 2\alpha$ $\alpha=45°$	$(1-\nu_{cr})<\varepsilon$	$\nu_u=1$ $\alpha=45°$	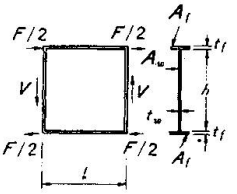
 $\lvert\sigma_1-\sigma_2\rvert=\sigma_{wY}$ $\sigma_2=-\tau_{cr}\sin 2\alpha$ $\alpha<45°$	$1-\frac{\lambda+\nu_{cr}(1+\lambda\nu_{cr})}{\sqrt{\lambda^2+(1+\lambda\nu_{cr})^2}}<\varepsilon\leq(1-\nu_{cr})$	$\nu_u=\frac{(1-\varepsilon)\nu_{cr}+\sqrt{1+\nu_{cr}^2-(1-\varepsilon)^2}}{1+\nu_{cr}^2}$ $\tan\alpha=\frac{\nu_{cr}+\sqrt{1+\nu_{cr}^2-(1-\varepsilon)^2}}{2-\varepsilon}$	$\lambda=\ell/h$: Aspect ratio α : Inclination of tension field σ_1, σ_1' : Principal stress (tension) σ_2 : Principal stress (comp.) σ_{wY} : Yield stress of web σ_{fY} : Yield stress of flange τ_{cr} : Web buckling stress $\varepsilon=\frac{8}{\lambda^2}\frac{t_f}{h}\frac{A_f\sigma_{fY}}{A_w\sigma_{wY}}$ $\nu_{cr}=\tau_{cr}/\tau_{wY}$ $\nu_u=V_u/A_w\tau_{wY}$
 $\lvert\sigma_1'-\sigma_2\rvert=\sigma_{wY}$ $\sigma_1'>\sigma_1$ $\alpha<45°$	$\varepsilon\leq 1-\frac{\lambda+\nu_{cr}(1+\lambda\nu_{cr})}{\sqrt{\lambda^2+(1+\lambda\nu_{cr})^2}}$	$\nu_u=\sqrt{\lambda^2+(1+\lambda\nu_{cr})^2}-(1-\varepsilon)\lambda$ $\tan 2\alpha=\frac{1+\lambda\nu_{cr}}{\lambda}$	

In Table 2.1.1. υ_{cr} is nondimensionalized shear buckling stress of web panel, and is given by formula (2.1.1.).

$$\upsilon_{cr}=\frac{K_s\pi^2}{12(1-\nu^2)}\left(\frac{E}{\tau_{wY}}\right)\left(\frac{t_w}{h}\right)^2,\quad \upsilon_{cr}\leq 0.5$$
$$=1-\frac{3(1-\nu^2)}{K_s\pi^2}\left(\frac{\tau_{wY}}{E}\right)\left(\frac{h}{t_w}\right)^2,\quad \upsilon_{cr}>0.5 \qquad (2.1.1)$$

where ν : Poisson's ratio, E: Young's modulus,

τ_{wY} : Yield stress of web $=\sigma_{wY}/2$ (Tresca's yielding condition is used in this theory).

K_s is a buckling coefficient depend on aspect ratio λ and constraint conditions along periphery of the panel. It seems appropriate to consider that the web is fixed along the flanges and simply supported along the vertical stiffeners, and under this condition Ostapenko gives the following formula[4]

$$K_s=\frac{5.34}{\lambda^2}+\frac{6.55}{\lambda}-13.71+14.10\lambda,\quad \lambda\leq 1.0$$
$$=8.98+\frac{6.18}{\lambda^2}-\frac{2.88}{\lambda^3},\quad \lambda>1.0 \qquad (2.1.2.)$$

In Table 3.1.1., ε is a parameter related to the effect of flange plate stiffness, and is given for any shape of flange cross section as,

$$\varepsilon=\frac{M_P^f}{\ell^2 t_w\sigma_{wY}} \qquad (2.1.3.)$$

where M_p^f is full plastic moment of flange itself.

formulas for specified sections are given in Table 2.1.2.

Table 2.1.2. ε -formulas for Specific Section of Flange Plate

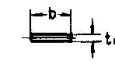	$\frac{1}{4}\frac{bt_1^2}{l^2 t_w}\left(\frac{\sigma_{fY}}{\sigma_{wY}}\right)$
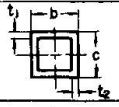	$\frac{1}{2}\frac{2bct_1+c^2t_2}{l^2 t_w}\left(\frac{\sigma_{fY}}{\sigma_{wY}}\right)$ $t_1 \ll b$, $t_2 \ll c$
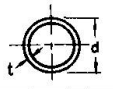	$\frac{d^2 t}{l^2 t_w}\left(\frac{\sigma_{fY}}{\sigma_{wY}}\right)$ $t \ll d$
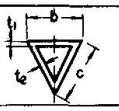	$\frac{2-\sqrt{2}}{3}\frac{1}{l^2 t_w}\left[\frac{(3bt_1-ct_2)c^2}{\sqrt{(b/2)^2+c^2}}+4ct_2\sqrt{(b/2)^2+c^2}\right]\left(\frac{\sigma_{fY}}{\sigma_{wY}}\right)$ $t_1 \ll b$, $t_2 \ll c$

Comparison of the theoretical values with the test results have already been reported at the 8th congress of IABSE in New York[2]

(2) Bending Strength of Plate Girders

Fujii has introduced the following theoretical formulas for calculating the ultimate bending strength on the assumption of lateral buckling of plate girder being prevented[1][3]

$$m_u = m_{cr} + \beta(1 - m_{cr}), \quad m_{cr} \leq 1.0$$
$$= \frac{f_s(m_{cr}-1)+(1-\xi)}{m_{cr}-\xi} \leq f_s, \quad m_{cr} > 1.0 \qquad (2.1.4.)$$

where $m = M/M_y$: nondimensionalized moment
My: flange yield moment
u : suffix for ultimate
cr : suffix for web-buckling
fs : shape factor used in plastic design

$$\xi = 2.42\left(\frac{t_w}{h}\right)\sqrt{\frac{E}{\sigma_Y}}$$

in this case $\sigma_{wY} = \sigma_{fY} = \sigma_Y$

In eq. (2.1.4.), κ_m is calculated as a simply supported rectangular plate subjected to inplane bending and is given as follows,

$$m_{cr} = \frac{K_m \pi^2}{12(1-\nu^2)}\left(\frac{t_w}{h}\right)^2\left(\frac{E}{\sigma_Y}\right)$$

$$K_m = 15.87 + 1.87/\lambda^2 + 8.6\lambda^2, \quad \lambda \leq 2/3 \qquad (2.1.5.)$$
$$= 23.9 \qquad \lambda > 2/3$$

β , in eq. (2.1.4.), is a parameter with the effective bredth of buckled web, and is given by the following formula[3]

$$\beta = 1 - \frac{(1-\xi)^2}{4(1+2A_f/A_w)} \quad \frac{(1-\xi)^3}{2(1+6A_f/A_w)} \qquad (2.1.6.)$$

where At : sectional area of flange
Aw : sectional area of web

Relations between buckling moment and ultimate moment given by eq. (2.1.4.) are graphically shown in Fig. 2.1.1.

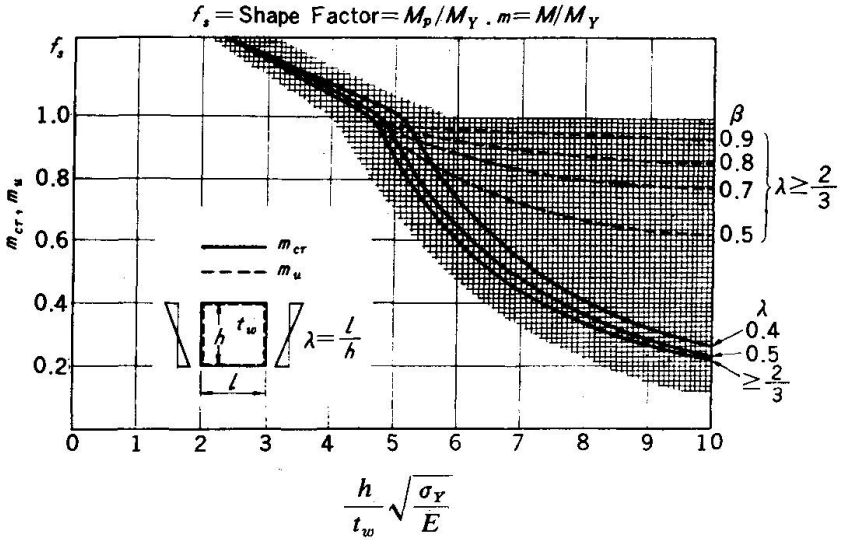

Fig. 2.1.1. Relation between Nondimensionalized Buckling Moment and Ultimate Moment

For hybrid girders, Fujii proposed to modify the results, in eqs. (2.1.4.) (2.1.5.) (2.1.6.) assuming $\sigma_Y = \sigma_{fY}$ by multiplying a correcting factor C_m; the ratio of the full plastic moment of the hybrid section to the assumed ($\sigma_Y = \sigma_{fY}$) full plastic moment,

namely,

$$M_u = C_m \, m_u \, M_Y \qquad (2.1.7.)$$

where $M_Y = S\sigma_{fY}$

S = section modulus

$$C_m = \frac{1 + \frac{t_f}{h} + \frac{1}{4}\frac{\sigma_{wY}A_w}{\sigma_{fY}A_f}}{1 + \frac{t_f}{h} + \frac{1}{4}\frac{A_w}{A_f}}$$

Comparison between theoretical and experimental results is shown in Table 2.1.3. and it shows good coincidence between them.

Table 2.1.3. Comparison of the theoretical values with the experimental results

Ref. No.	Girder No.	Experimental Values								Theoretical Values			
		λ	h/t_w	A_w s.i.	A_f s.i.	σ_Y k.s.i.	M_Y kips-inch	M_p kips-inch	M_u^x kips-inch	$\frac{h}{t_w}\sqrt{\frac{\sigma_Y}{E}}$	m_{cr}	m_u	$\frac{M_u^y}{M_u^x}$
Lehigh Univ.[5]	G2–T1	1.5	185	13.5	9.40	38	2.23×10^4	2.42×10^4	2.02×10^4	6.60	0.495	0.962	0.94
	G2–T2	0.75	"	"	"	"	"	"	2.16×10^4	"	"	"	1.01
	G4–T1	1.5	388	64.5	9.40	38	1.96×10^4	2.12×10^4	1.77×10^4	13.8	0.113	0.928	0.98
	G4–T2	0.75	"	"	"	"	"	"	1.88×10^4	"	"	"	1.03
Texas Univ.[6]	41540	1.0	147	8.82	4.187	*1 105/41.6	*2 2.15×10^4	1.94×10^4	1.63×10^4	8.76	0.282	0.916	1.04
	42540	1.0	"	"	4.173	"	"	1.93×10^4	1.65×10^4	"	"	"	1.06
				cm^2	cm^2	kg/cm^2	kg-cm	kg-cm	kg-cm				
Konishi and Others[7]	A	1.0	267	54.0	28.8	28.1	1.28×10^7	1.43×10^7	1.16×10^7	9.75	0.228	0.892	1.02
	G	1.0	200	72.0	28.8	50.0	2.47×10^7	2.83×10^7	2.40×10^7	9.76	0.227	0.873	1.11
Akita and Fujii[1]	B–1	0.988	212	20.4	14.7	27.0	3.25×10^6	3.56×10^6	3.19×10^6	7.61	0.373	0.945	1.04
	B–2	0.975	155	14.9	14.7	27.0	2.27×10^6	2.43×10^6	2.14×10^6	5.56	0.698	0.988	0.96

*1 σ_{fy}/σ_{wy}

*2 $M_y = S\sigma_{xy}$ where S is section modulus.

(3) Interaction Curve under Combined Bending and Shear

Fujii has introduced the following interaction formulas under combined bending and shear[1][3]

In the case where the web buckling is prevented, interaction formulas are given as follows,

$$M = M_{fp} + M_{wp}\sqrt{1-(V/V_p)^2}\ ,\quad M \geq M_{fp} \qquad (2.1.8.)$$

$$V = V_p \qquad M < M_{fp}$$

where

$M_{wp} = \frac{1}{4}h^2 t_w \sigma_{wY}$: Plastic moment shared by web.

$M_{fp} = (h+t_f)A_f\sigma_{fY}$: Plastic moment shared by flange.

$V_p = A_w\tau_{wY}$: Plastic shear force.

This may be diagrammatically shown by a chain line A'B'C' in Fig. 2.1.2. When a plate girder is subjected to bending moment only, the ultimate moment Mu (the point A in Fig. 2.1.2.) represents the critical value. When the web has just buckled and the tension field does not grow yet, the flanges can bear the moment denoted Mfp. The point B corresponds to this critical value. When the flanges yield under the combined bending moment and compressive force caused by the tension field action, a contribution of flange stiffness on ultimate shear force can not be expected, and this corresponds to the point C. Vu represents the critical point under shear force only. In this case, the plate girder cannot bear the bending moment because the flanges collapse at the same time.

The interaction curve can be approximated on the safe side by connecting the points A.B. C. and D. by a folded line.

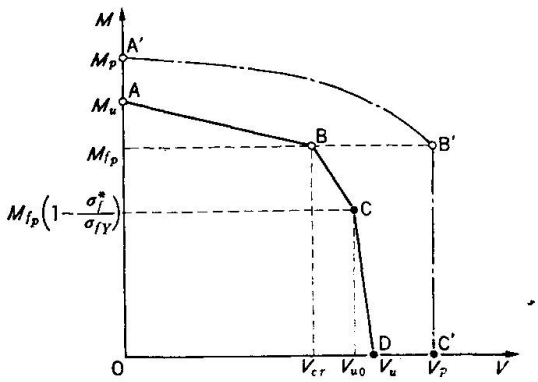

Fig. 2.1.2. Interaction Curve

At A, $M_A = M_u$, $V_A = 0$ (2.1.9.)

At B, $M_B = M_{fp}$, $V_B = V_{cr}$, (2.1.10.)

At C, $M_C = M_{fp}\left(1 - \frac{\sigma_f^*}{\sigma_{fY}}\right)$ $V_C = V_{uo}$, (2.1.11.)

where Vuo is the ultimate shearing force when ϵ is zero, and σ_f^* is compressive stress in the flanges by the action of tension field.

They can be obtained as follows[1]

$$\lambda > \frac{1}{\tau_{cr}} \frac{1-\tau_{cr}^2}{1+\tau_{cr}^2} \quad , \quad \tau_{uo} = \frac{2\tau_{cr}}{1+\tau_{cr}^2}\tau_p$$
$$\frac{\sigma_f^*}{\sigma_{fY}} = \frac{A_w \sigma_{wY}}{2A_f \sigma_{fY}} \frac{1-\tau_{cr}^2}{1+\tau_{cr}^2} \qquad (2.1.12.)$$

$$\lambda \leq \frac{1}{\tau_{cr}} \frac{1-\tau_{cr}^2}{1+\tau_{cr}^2} \quad , \quad \tau_{uo} = \left(\sqrt{\lambda^2 + (1+\lambda\tau_{cr})^2} - \lambda\right)\tau_p$$
$$\frac{\sigma_f^*}{\sigma_{fY}} = \frac{A_w \sigma_{wY}}{4A_f \sigma_{fY}} \left\{1 + \lambda\tau_{cr} - \frac{\tau_{cr}(1+\lambda\tau_{cr})}{\sqrt{\lambda^2 + (1+\lambda\tau_{cr})^2}}\right\} \qquad (2.1.13.)$$

At D, $M_D = 0$, $V_D = V_u$, (2.1.14.)

The results of girder tests conducted by Basler, Thürliman and others[5] and Cooper and others[8] under combined bending and shear are summarized in Table 2.1.4. These experimental values are compared with the theoretical interaction curves in Fig. 2.1.3. – 2.1.8[3]. The experimental values are in fairly good coincidence with the theoretical values and the interaction curves are on the safe side.

Table 2.1.4. Test Results of Girders under combined Shear and Bending

Ref. No.	Girder No.	λ	h/tw	Aw s.i.	σwY k.s.i.	Af s.i.	σfY k.s.i.	ε	Vp kips	My kips-inch	Mp kips-inch	V_u^{ex} kips	M_u^{ex} * kips-inch
Lehigh Univ. [5]	G8–T1	3.0	254	9.85	38.2	8.99	41.3	0.013	188	21,900	23,600	85.0	6,380
	G8–T3	1.5	"	"	"	"	"	"	"	"	"	116.5	13,100
	G8–T4	1.0	"	"	"	"	"	0.119	"	"	"	129.5	16,200
	G9–T1	3.0	382	6.55	44.5	9.00	41.8	0.017	146	21,100	22,700	48.0	3,600
	G9–T2	1.5	"	"	"	"	"	0.069	"	"	"	75.0	2,810
	G9–T3	"	"	"	"	"	"	"	"	"	"	79.0	8,890
	E2–T1	3.0	99	25.35	34.9	25.4	38.1	0.0178	443	48,500	54,100	377.5	47,200
	E2–T2	1.5	"	"	"	"	"	0.0713	"	"	"	378.5	42,500
	E4–T2	0.75	"	"	"	"	"	0.261	"	"	"	317	41,600
	E4–T3	0.5	"	"	"	"	"	0.587	"	"	"	322.5	44,300
Lehigh Univ. [8]	H1–T1	3.0	127	19.65	108.1	34.4	106.1	0.030	1,060	207,200	216,000	630	47,250
	H1–T2	1.5	"	"	"	"	"	0.060	"	"	"	769	28,900
	H2–T1	1.0	128	19.5	110.2	35.4	107.1	0.284	1,075	214,600	224,100	917	114,600
	H2–T2	0.5	"	"	"	"	"	1.136	"	"	"	1,125	154,700

* Values at midspan of failure panel.

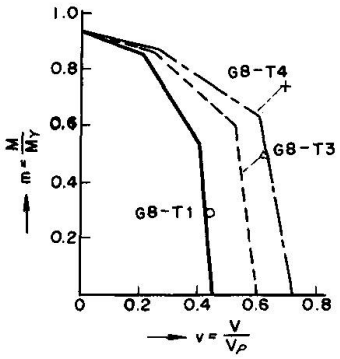

Fig. 2.1.3

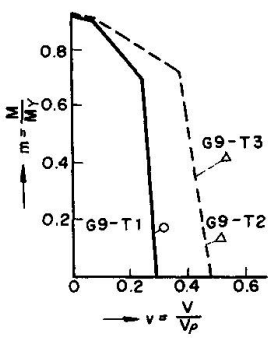

Fig. 2.1.4

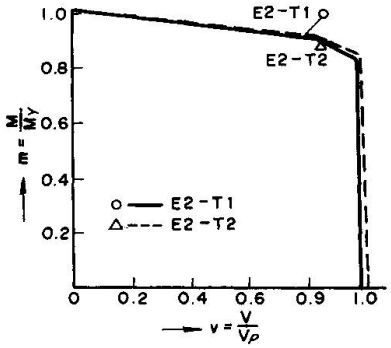

Fig. 2.1.5

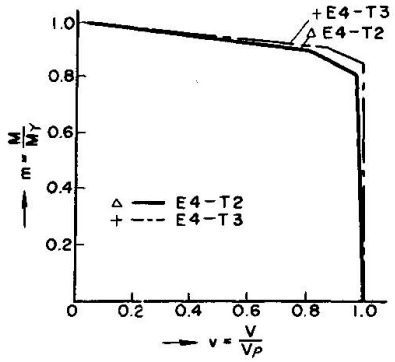

Fig. 2.1.6

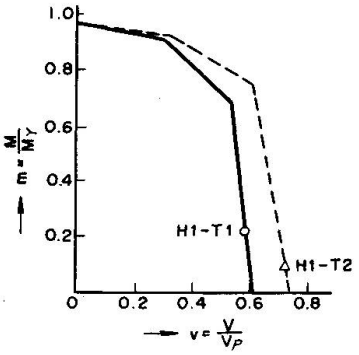

Fig. 2.1.7

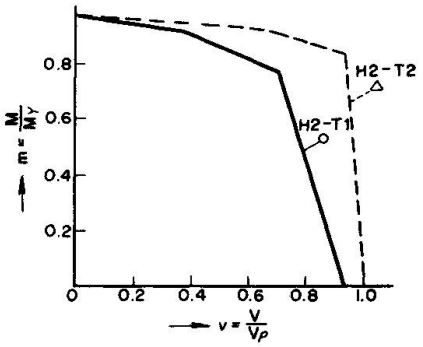

Fig. 2.1.8

References:

1) Y. Akita & T. Fujii: "Minimum Weight Design of Structures based on Buckling Strength and Plastic Collapse (1st and 2nd Report)". Selected papers from the Journal of the Society of Naval Architects of Japan Vol. 2, 1969.

2) T. Fujii: "On an Improved Theory for Dr. Basler's Theory" The Final Report of the 8th Congress of IABSE.

3) T. Fujii: "On the Ultimate Strength of Plate Girders. Japan Shipbuilding & Marine Engineering, Vol. 3, No. 3, May 1968.

4) C. Chern & A. Ostapenko: "Ultimate Strength of Plate Girders under Shear (Unsymmetrical Plate Girders)". Fritz Engineering Laboratory Report No. 328.7, August 1969.

5) K. Basler, B. Thurliman, and others: "Web Buckling Test on Welded Plate Girders" Bulletin No. 64, Welding Research Council, N. Y., 1960.

6) H. Toyoda: "Static Behaviour of Hybrid Plate Girders" Thesis for the Degree of M.S. University of Texas, Janu. 1967.

7) I. Konishi and others: "Theories and Experiments on the Load Carrying Capacity of Plate Girders" Report of Research Committee of Bridges, Steel Frames and Welding in Kansai District in Japan, July 1965 (in Japanese)

8) P. B. Cooper and others: "Welded Constructional Alloy Steel Girders" Proc. of A.S.C.E. ST1, 1964.

2.2 Lateral Collapse of Plate Girders in Bending

Ultimate strength of plate girders in bending would be governed by the following collapse mechanisms, that is, (1) excessive deformations of girders in the plane of bending, (2) local failures of the compression flange such as vertical buckling of the flange into the web and torsional buckling of the flange plate, and (3) lateral buckling of the compression flange between the unsupported length of the flange.

In this report a study which is related to the above item (3) is carried out by Fukumoto in order to clarify the interaction between the lateral collapse load of the girders and stress concentration in the compression flange and a portion of the web adjacent to it which is caused by a redistribution of the web stress in post buckling range. Comparisons are also made between the inelastic lateral buckling theory and the test results of girders with high strength steels of SM 50 (nominal yield stress σ_Y=3,200 kg/cm^2) and HT 80 (σ_Y=7,000kg/cm^2).

The Test Girders

Since the objective of this investigation is to study the interaction between the buckled web and the lateral collapse of girders under pure bending, no lateral bracings are provided for the test girders except at the both ends where the loading box beams are connected by the high strength bolts. The end conditions of test girders are, therefore, clamped laterally in the plane of the flange plates.

The detailed dimensions of the test girders are given in Fig. 2.2.1. and Table 2.2.1. Girders A and B are of SM 50 steel, girders C,D,E and F are of HT 80 and girder G is a hybrid girder with SM 50 steel in the web and HT 80 in the flange plates. The number of panels between the transverse stiffeners are two for girders D and F, and the others have three panels.

All seven girders are tested under pure bending in the setup as shown in Fig. 2.2.2. End box beams are prevented laterally at the sections where two 75 ton capacity hydraulic jacks applied loads.

Instrumentations

Fig. 2.2.3. shows the location of the strain gages to the web and flange. In the web orthogonal pairs of gages are mounted on either side of the web at the mid cross-section of each panel in order to differentiate bending and membrane strains. Gages to the flange are placed to differentiate stresses in the compression flange due to in-plane and out-of-plane bending of the girders.

The vertical and lateral deflections of the flanges are obtained through the dial gages. A dial gage rig is made to obtain the out-of-plane deformations of the web. Rotation of the compression flange is read using a clinometer for surveying. The position of measuring deflections is also shown in Fig. 2.2.3.

Test Results and Discussions

TENSION COUPON TESTS : Two coupons are cut from each slab thickness. Average values of static yield stress for each slab thickness are as follows:

SM 50	σ_Y = 4690 kg/cm^2	for t = 6 mm
	σ_Y = 3810 kg/cm^2	for t = 8 mm
	σ_Y = 3240 kg/cm^2	for t = 10 mm
HT 80	σ_Y = 6610 kg/cm^2	for t = 6 mm
	σ_Y = 7850 kg/cm^2	for t = 10 mm

LOAD-DEFORMATION CURVES : The absolute girder deflections including lateral web deflections are measured at the mid cross-sections of each panel of the girders. The deformations are recorded for the initial distorsions of the girders and for a number of loads.

Fig. 2.2.4.(a) shows the absolute deformations at the mid cross-sections of the central and adjacent side panels of girder E. Deformations are shown under the four moment values. The graphs of deformations are composed of the relative deflection of the web out-of-its plane with the flange displacements in vertical, horizontal and rotational directions.

The relative deflection of the web starts for loads from the initial distortions of the web, and with the load increased the web buckled shapes become large to continue until lateral collapse occurs in the compression flange at the maximum moment. As can be seen from this figure, the web buckled pattern in each panel become obvious with the increased loads. In the central panel the direction of the relative web deflection is opposite to the lateral displacement of the compression flange and thus the lateral movement of the flange becomes small compared to the one in the side panel due to the resultant lateral forces transmitted to the flange along the web-flange weld line. In this figure load versus vertical deflection at the span center is compared with the deflection of $v = ML^2/8EI$ by conventional beam theory.

Fig. 2.2.4.(b) shows the deformations of girder C. In this case the direction of the relative web deflection and the lateral displacement of the compression flange is the same in the central panel, but in the side panel the lateral displacement of the flange is considerably small because of the web deflection being opposite to it.

STRAIN DISTRIBUTION AND EFFECTIVE BREDTH OF THE WEB : Fig. 2.2.5. shows the distributions of the mean web strains along the sections where the deformations are measured. The mean strains are the average of the values obtained from gages on either side of the web. In Fig. 2.2.5. the linear strain distributions predicted by conventional beam theory are also shown by light lines for girders A and C, respectively. A redistribution of mean strains in the compression zone of the web is observed with the increasing loads and, consequently, a portion of the compression stress in the web are transferred to the compression flange while the girders deform laterally with the loads. The compression flange and an adjacent web portion, thus, carry bending stress which exceeds that predicted by beam theory.

Girder A was loaded up to 41.4 t-m and then the girder was completely unloaded in order to replace a damaged angle of the girder end fixtures. The presence of residual horizontal displacement of 21.5 mm in the compression flange at the span center was recorded after unloading and, therefore, in the second test the lateral collapse of the girder was observed at the relatively early stage of loading. This result may be explained in Fig. 2.2.5. in which high strain concentration can be seen in the compression flange and an adjacent web portion.

If the first moment of the compression stresses in the web and flange (Fig. 2.2.6(a)) about the neutral axis is made equal to that of the linear stresses in the effective portion (Fig. 2.2.6.(b)), the effective bredth h_e may be calculated by,

$$\sum_i \sigma_i \Delta A_i h_i = \frac{\sigma_c}{h+t} \left\{ \frac{w}{3} \left[h^3 - (h-h_e)^3 \right] + bt\left(h + \frac{t}{2}\right)^2 \right\} \qquad (2.2.1)$$

in which σ_c is the measured fiber stress in the compression flange.

Fig. 2.2.7. shows h_e/h versus M/M_{max} curves for all the test girders. The ratios of h_e to the web thickness are also taken in the ordinate. When the bending moments reach the maximum moments at which the girders fail laterally, the effective bredth may become (30 – 35) times the web thickness.

Stress concentration in the flange could be estimated using the modified stress distribution as shown in Fig. 2.2.6.(b). For HT 80 steel girders, the stress concentration factors of σ_c (Fig. 2.2.6.(b)) against the

fiber stress calculated by conventional beam theory are equal to 1.09, 1.05 and 1.03, for h_e/h=0.4, 0.5 and 0.6 in Fig. 2.2.7., respectively.

ULTIMATE MOMENT : A summary of all ultimate moments, M_{max}, is given in Table 2.2.2. The failure mode of the girders is of the lateral instability of the compression flange. A hybrid girder G has the same cross-sectional dimensions of girder C. These two girders delivered almost the same ultimate loads regardless of the different yield stresses in the web.

The yield moment M_y which is the moment initiates nominal yielding in the extreme fiber, and the critical moment M_{wcr} which is the ideal buckling moment of an isolated web panel with the panel's aspect ratio under simply supported on all sides are given in Table 2.2.2. The overall buckling moment M_{ocr} and lateral buckling moment M_{cr} which will be obtained in the subsequent sections are also listed.

OVERALL BUCKLING OF GIRDERS : The web buckling problem in bending is treated herein as the simultaneous buckling of a plate girder, that is, combined web buckling and flange torsional and lateral buckling. Boundary conditions of web plate are simply supported along vertical stiffeners, clamped along tension flange and elastic support in torsion and lateral displacement along the compression flange. Normal stress in flange due to bending of girder is taken into account for the analysis and the reduction of apparent torsional rigidity and horizontal flexural rigidity of flange due to axial compression are considered.

The buckling coefficients are obtained by solving the equation of

$$\nabla^2\nabla^2 W = \frac{\sigma_0}{D}\left(1-\alpha\frac{y}{d}\right)W_{xx} \qquad (2.2.2.)$$

with the boundary conditions of (see Fig. 2.2.8)

$w = 0,\ w_y = 0$ for y = 0 (along tension flange)

$$\left.\begin{aligned} BW_{xxxx} &= D\left[W_{yyy} + (2-\nu)W_{xxy}\right] - A_f\sigma_0(1-\alpha)W_{xx} \\ D(W_{yy} + \nu W_{xx}) &= C\left[1 - \frac{\sigma_0(1-\alpha)I_P}{C}\right]W_{xxy} \end{aligned}\right\} \text{ for y=b (along compression flange)}$$

And the deflection surface is assumed as [1]

$$W = \sum_m \left[\sum_n a_n\left(\frac{y}{d}\right)^n\right]\sin\frac{m\pi x}{a} \qquad (2.2.3.)$$

Relationships between the simultaneous buckling strength and the three independent buckling modes, torsional buckling of flange, web buckling and lateral buckling of flange, are compared with the parameters of aspect ratios and slenderness ratios of web, cross-sectional areas of flange and web, torsional rigidity of flange, flexural rigidity of flange and web.

The curves corresponding to this method are shown as the overall buckling curves in Figs. 2.2.9.(a) and (b) for test girders with HT 80 steel. For $L/r>90$ approximately, the curves become close to the lateral buckling curves. Comparisons of the test results with the overall buckling curves indicate that the curves cannot predict the lateral collapse for the range where the overall buckling would be governed by the web buckling.

LATERAL BUCKLING STRENGTH : Lateral buckling strength of plate girders in bending was treated throughly in Ref. 2 in which the contributions of lateral bending of the flange plates with one sixth of the web and St. Venant torsion were discussed in detail.

Elastic lateral buckling strength curves for the test girders are shown in Figs. 2.2.9.(a) and (b) on the assumption that the distorsion of the girder cross section does not occur at the instance of buckling. Slenderness ratio for the minor axis of the girder cross section is taken in the abscissa.

Inelastic lateral buckling strength of girders with the residual stress pattern shown in Fig. 2.2.9.(a) is obtained and the results are shown in Figs. 2.2.9.(a) and (b). The assumptions used in the analysis are the same as those made in Ref. 3. From Figs. 2.2.9.(a) and (b) the test results for girders E to G are in good agreement with the inelastic lateral buckling curves.

If St. Venant torsion is neglected, elastic lateral buckling of doubly symmetrical I sections in bending may be written as

$$\frac{\sigma_{cr}}{\sigma_Y} = \frac{1}{\alpha^2} \qquad (2.2.4.)$$

in which $\alpha = \frac{1}{\pi}\sqrt{\frac{\sigma_Y}{E}}\frac{L}{\bar{r}}$ and $\bar{r}$ is the radius of gyration of the compression flange and one sixth of the web which is defined as

$$\bar{r}^2 = \frac{I_f}{A_f + \frac{1}{6}A_w} \quad \text{with} \quad I_f = \frac{b^3 t}{12} \qquad (2.2.5.)$$

Fig. 2.2.10. shows summary of the test results and the corresponding theoretical curves. α is taken in the abscissa. Elastic buckling curves for all the test girders can then be represented reasonably by Eq. (2.2.4.)

The basic column curve

$$\frac{\sigma_{cr}}{\sigma_Y} = 1 - \frac{\alpha^2}{4} \quad \text{for } 0 < \alpha < 2 \qquad (2.2.6.)$$

is plotted in Fig. 2.2.10. And the theoretical transition curve is also shown for the girders with a residual stress pattern as in Fig. 2.2.9.(a).

From this figure, lateral collapse of the test girders in bending may occur when the moments reach the strength estimated by the inelastic lateral buckling theory including residual stresses. However, overall buckling curve may not give adequate estimation of the problem when the web buckles in several half waves.

CONCLUSIONS:

The behavior of lateral collapse of plate girders in bending was investigated for SM 50 (σ_Y=3200 kg/cm^2) and HT 80 (σ_Y=7000 kg/cm^2) steels. At the early stage of loading, the lateral and torsional deformations of the girder flanges were observed together with the buckled patterns in each web panel. Lateral deflection curves of the compression flange at failure were influenced considerably by the direction of the buckled deformation of the web. Variations of the effective sections of the web with the loads during the lateral collapse were discussed. Lateral instability of the compression flange can be estimated satisfactorily by the inelastic lateral buckling theory neglecting St. Venant torsion.

References

1) H. Yonezawa and I. Mikami, "Elastic Buckling of Plate Girders from Pure Bending", Proc. of ASCE, Vol. 94, No. EM1, Feb., 1968

2) K. Basler and B. Thurlimann, "Strength of Plate Girders in Bending", Proc. of ASCE, Vol. 87, No. St 6, Aug., 1961

3) T.V. Galambos, "Structural Members and Frames" Prentice-Hall, 1968

Table 2.2.1. Dimensions of Test Girders

Girders	Steels	d (mm)	b (mm)	w (mm)	t (mm)	L_0(mm)	Number of Panels	a_1(mm)	a_2(mm)	Stiffeners (mm)
G–A	SM50A	1000	130	6	10	4100	3	1200	450	62 x 8
G–B	SM50A	1000	120	6	8	4100	3	1200	450	51 x 8
G–C	HT80	800	110	6	10	3300	3	900	350	52 x 8
G–D	HT80	800	110	6	10	2800	2	1000	–––	52 x 8
G–E	HT80	800	130	6	10	3300	3	900	350	62 x 8
G–F	HT80	800	130	6	10	2800	2	1000	–––	62 x 8
G–G	Flange HT80 Web SM50A	800	110	6	10	3300	3	900	350	52 x 8

Table 2.2.2. Summary of Test Results and Reference Moments

Girders	Experimental	Theoretical			
	M_{max}	M_{wcr}	M_{ocr}	M_{cr}	M_y
G–A	43.6	38.5	52.7	53.8	71.7
G–B	41.0	32.8	40.2	50.5	72.3
G–C	64.4	40.4	55.2	65.1	113.9
G–D	83.4	39.9	55.2	81.1	113.9
G–E	94.8	44.8	64.1	90.8	126.2
G–F	105.1	44.2	64.1	94.6	126.2
G–G	65.5	40.4	55.2	65.1	–––

Unit in t-m

M_{wcr} : ideal buckling moment of an isolated web panel
M_{ocr} : overall buckling moment
M_{cr} : lateral buckling moment
M_y : yield moment

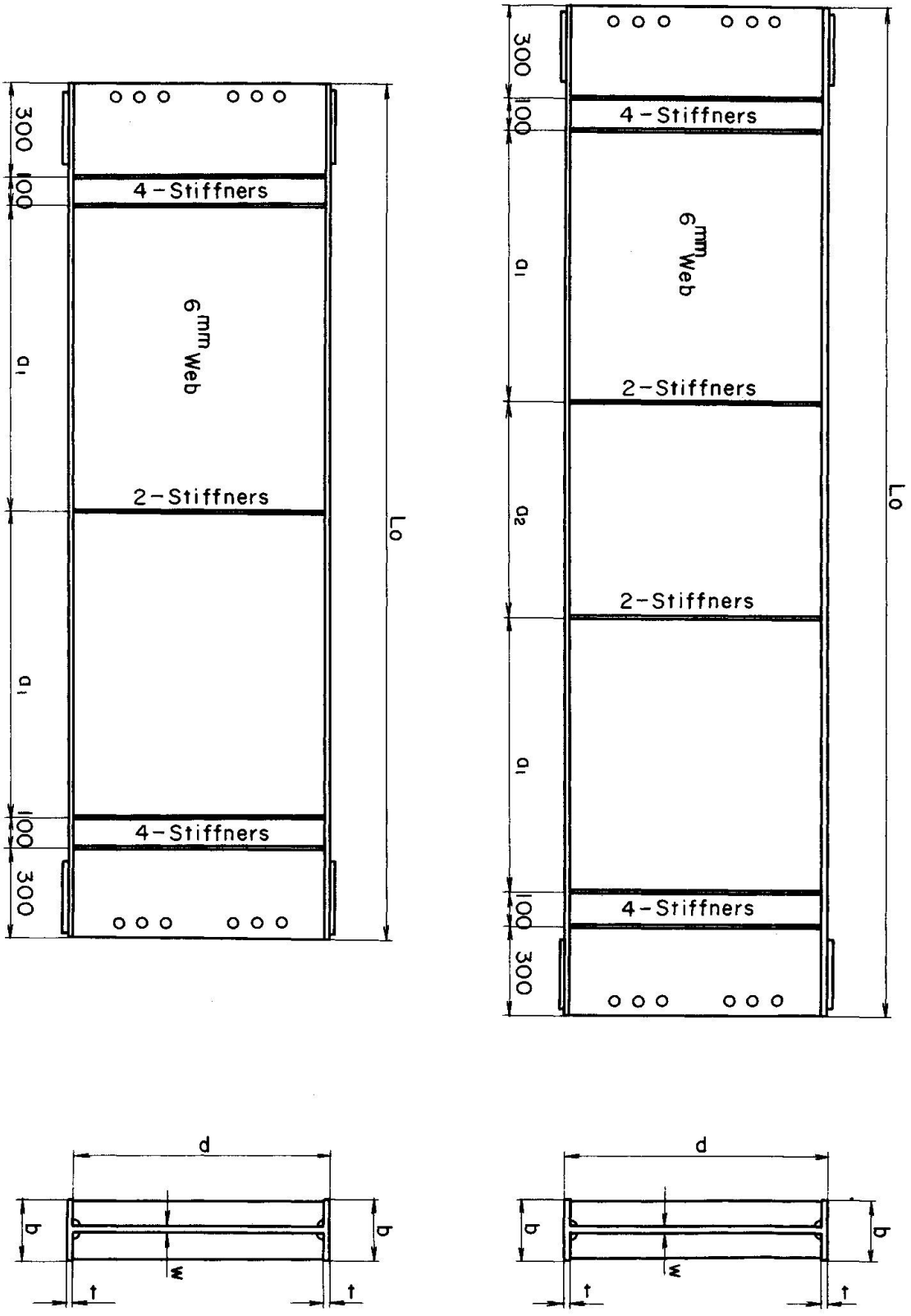

Fig. 2.2.1 Test Girders

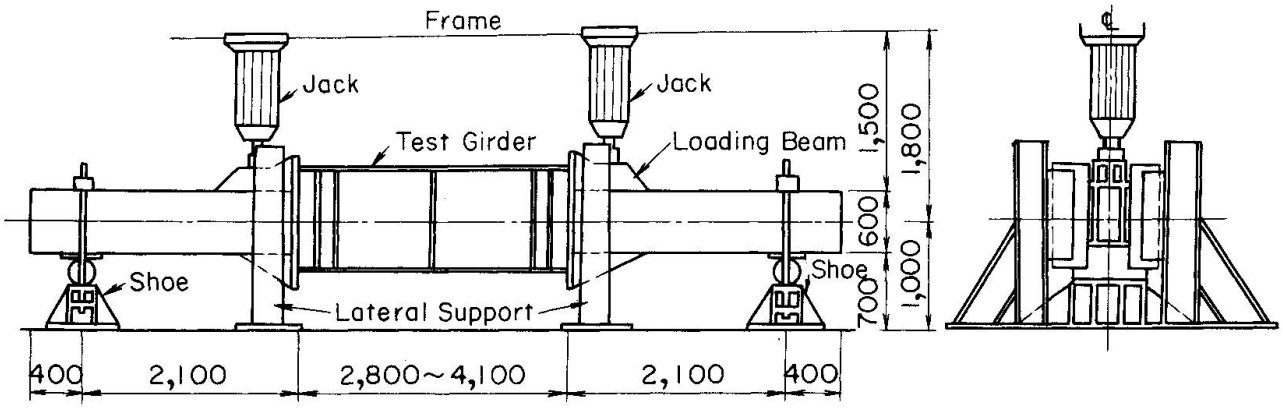

Fig. 2.2.2 Test Setup

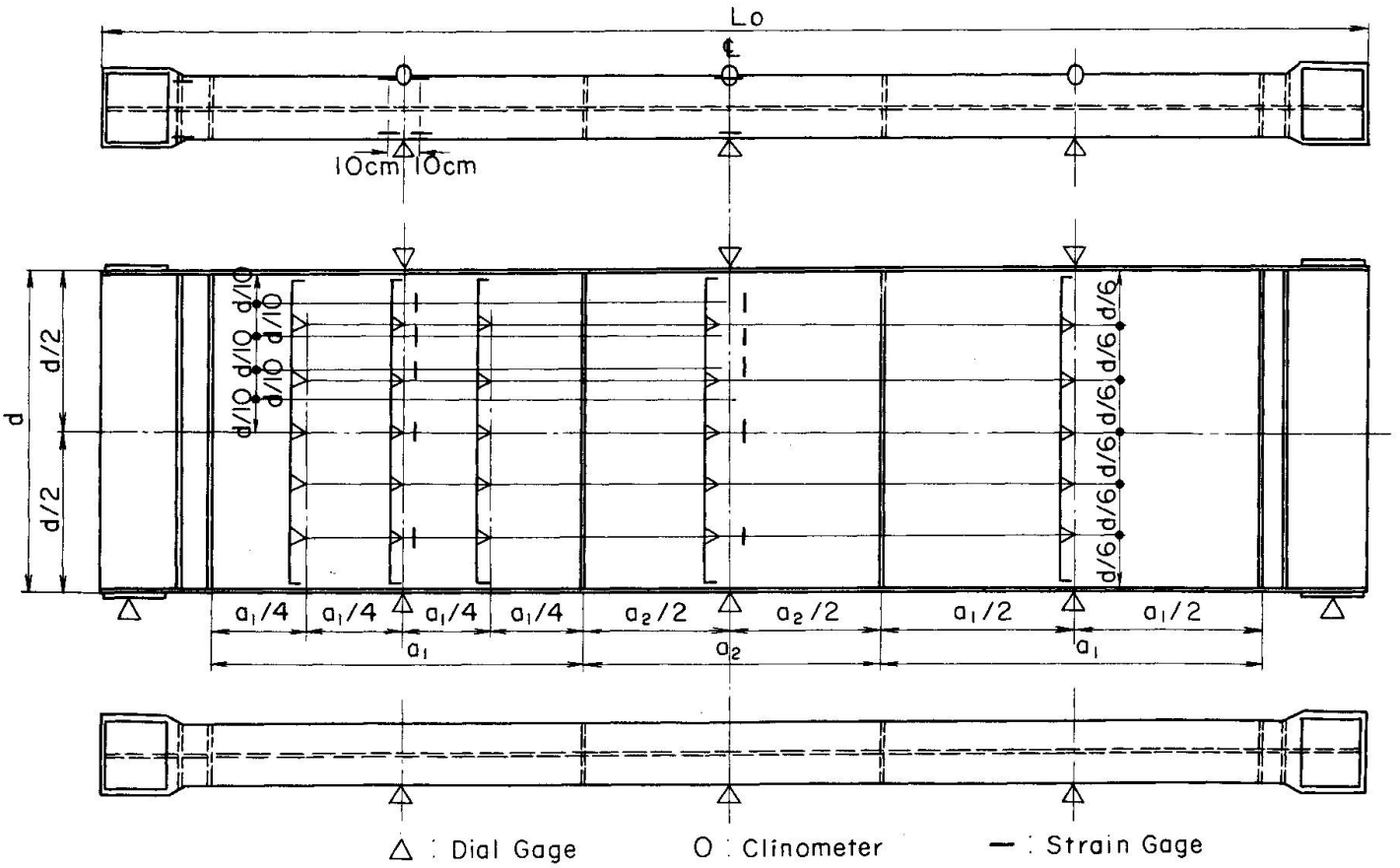

Fig. 2.2.3 Instrumentation

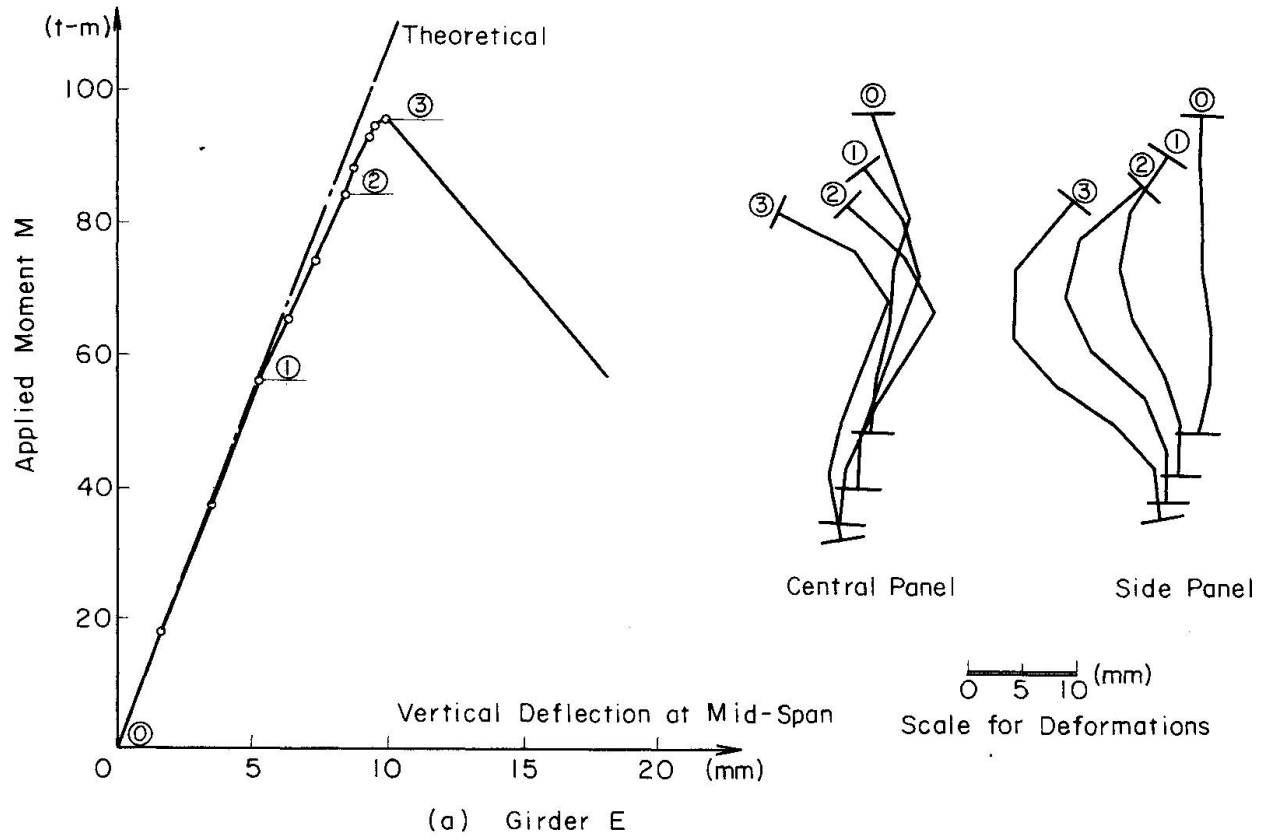

(a) Girder E

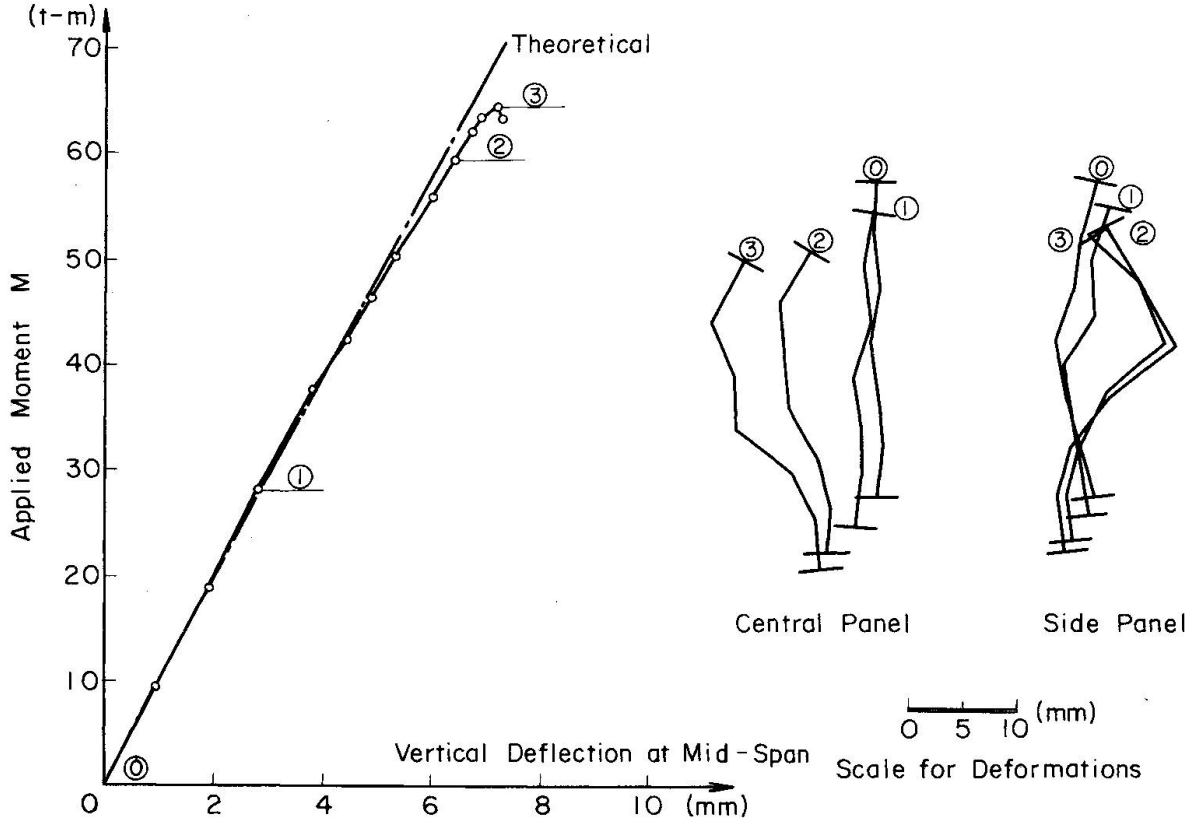

(b) Girder C

Fig. 2.2.4 Load – Deformation Relations

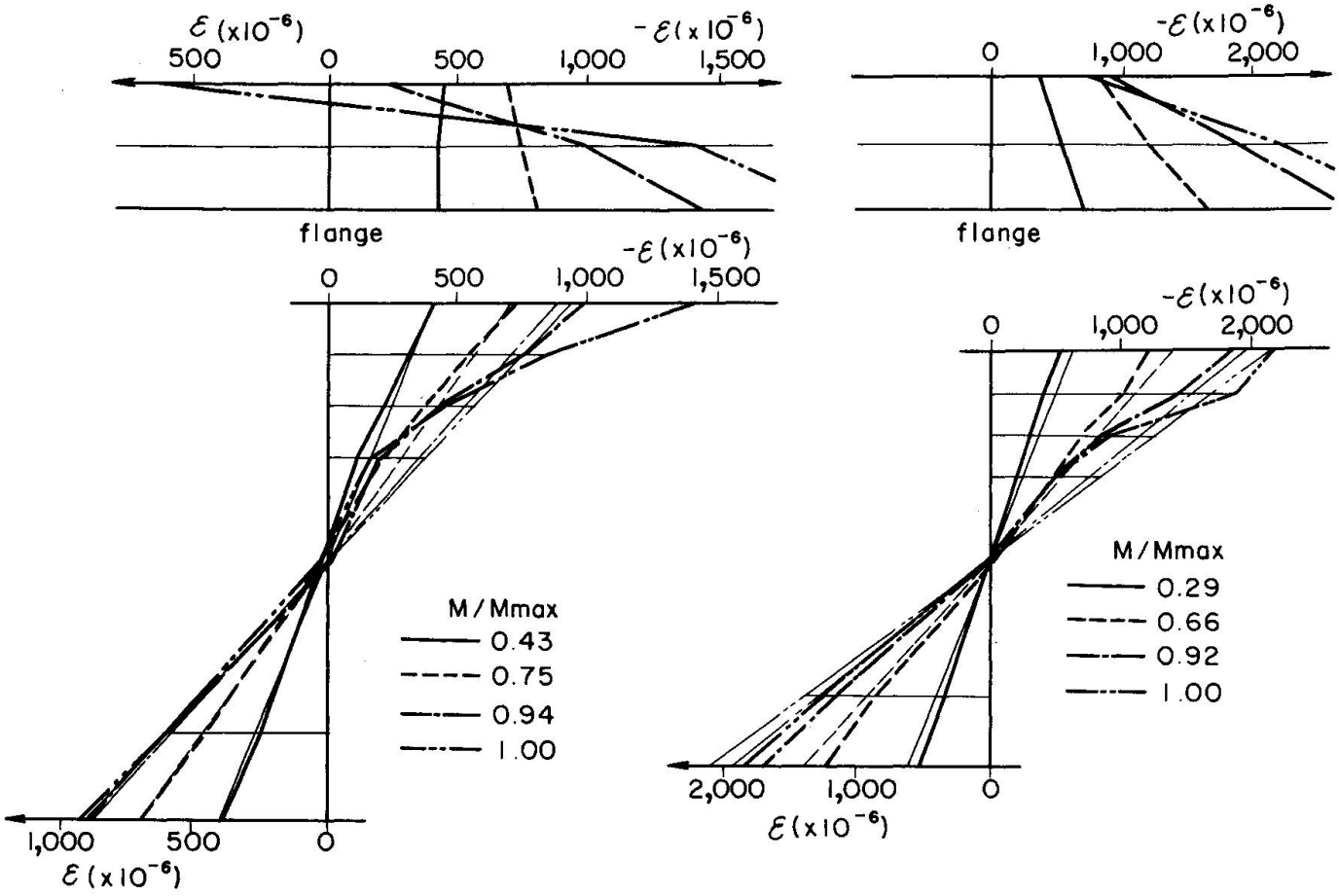

(a) Girder A (b) Girder C

Fig. 2.2.5 Strain Distribution at the Panel Center

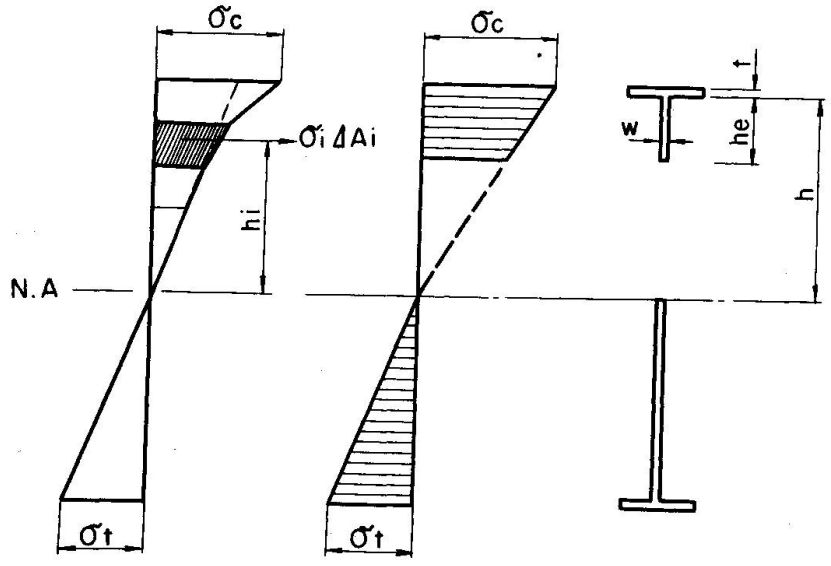

(a) (b)

Fig. 2.2.6 Modified Stress Distribution

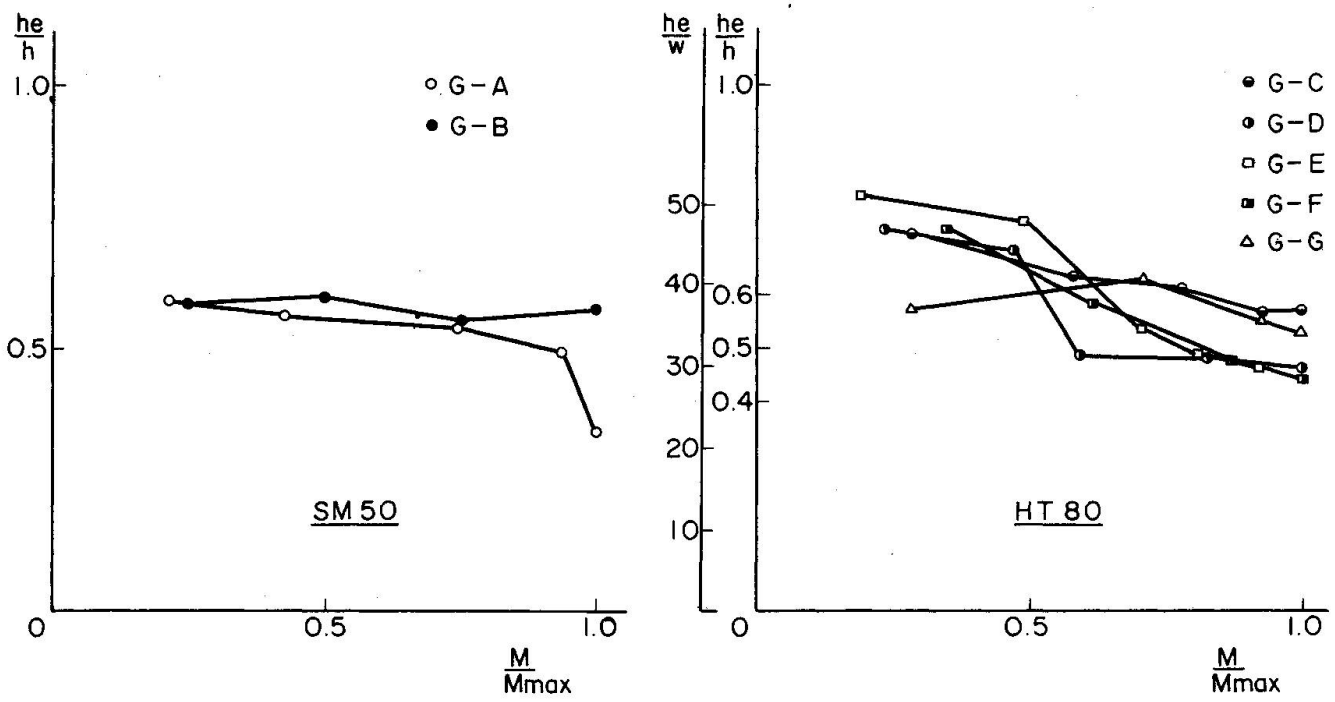

Fig. 2.2.7 Effective Bredth of Web

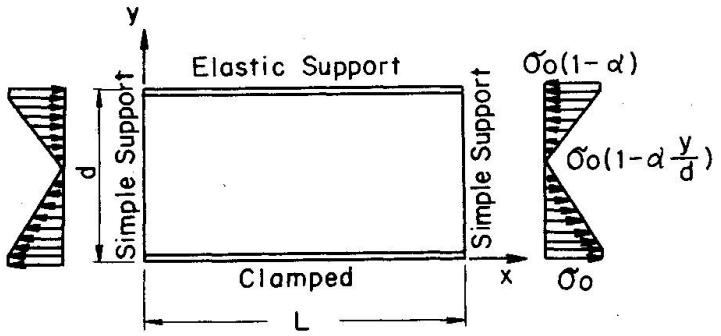

Fig. 2.2.8

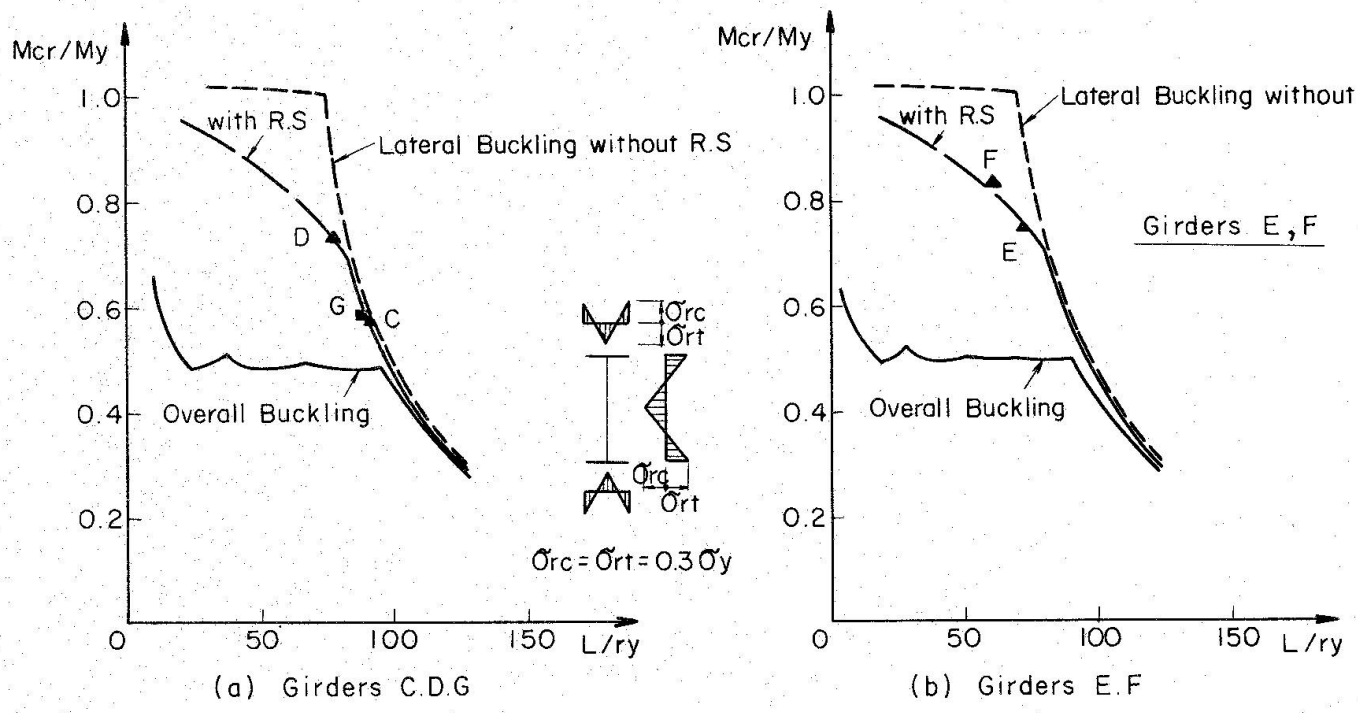

Fig. 2.2.9 Comparison of the Test Results with the Theories

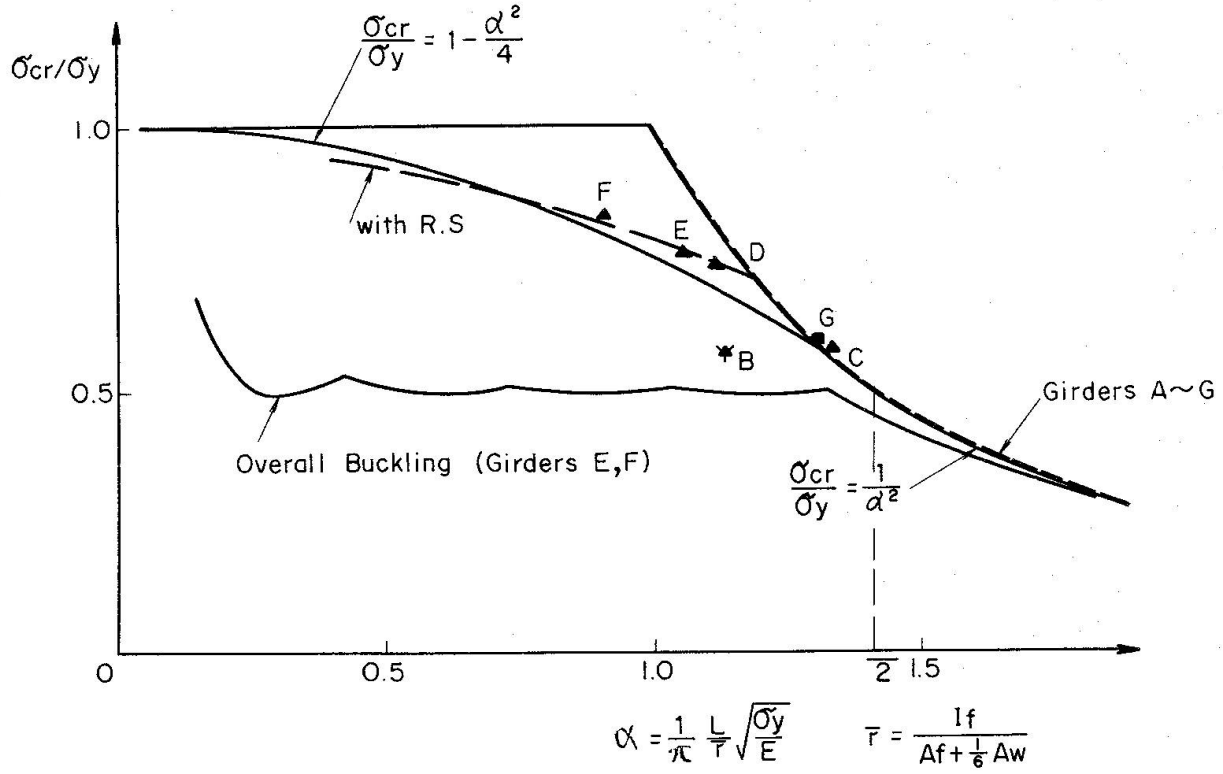

Fig. 2.2.10 Test Results and Theoretical Buckling Curves

2.3 Load-Deformation Characteristics of Plate Girders

With the increase of labor cost, there is a tendency that plate girder bridges of a relatively short span are shop-produced in large quantities. Strength of these mass-produced steel girders are studied from the two points of view; one is on the shear strength of welded built-up girders[1] and the other is on the moment carrying capacity of large size rolled I-profile beams[2]

From the economic point of view in fabrication of welded built-up girders with employment of automatic welding in mind, a design with no intermediate stiffener or a design with only horizontal stiffeners is preferred to that equipped with intermediate transverse stiffeners. Shear tests were performed by Nishino and Okumura on a series of full size plate girders with transverse stiffeners only at the supports and at the center of the test specimens where loading was applied. The depth to thickness ratios of the web plates made of a steel with yield strength of 40 kg/mm^2 ranged from 60 to 120.

The experimentally observed maximum loads exceeded the web buckling loads for all of the test girders, with exceptions of the girders with small depth-thickness ratios and failed by flange instability. Despite the comparatively small rigidity of the frameworks due to large aspect ratio of web panels of around 2.6 and in addition due to relatively smaller depth-thickness ratios of 120 at most, a large reserve of strengths above the buckling load was observed among the deeper girders, even for the girders failed by flange instability.

Although some of the design specifications restrict the use of web panels without intermediate vertical stiffeners except panels with thick plates, the tests revealed no particular ground for the restriction under static loading condition. The permissible shear stress specified in AASHO design specifications, one of the specifications which permit the use of this type of web panels, turned out to be very conservative for the test girders.

A horizontal stiffener placed at half the depth worked effectively to prevent premature buckling of the web due to shear force, suggesting a feasibility of an economical design of horizontally stiffened plate girders for shop-produced bridges in large quantities, in which no intermediate vertical stiffeners may be placed except at the points where heavy loads are concentrated.

The plastic collapse loads correlated well with the test results and represented best the experimentally obtained ultimate loads for all girders tested including the girders with d/t_w ratio of as large as 120.

Rolled I-beams in general have relatively thick web plates compared with welded built-up shapes of similar cross sectional properties and as a result the rolled shapes are inferior from the point of efficiency of cross sections. A study was carried out by Nishino and Okumura on large size rolled I-beams with the depth of 900 mm in order to study the magnitude and distribution of residual stresses inherent in the beams and their effect on the moment carrying capacity of the beams. It was found that the residual stresses present in the large size as-rolled beams are for large in magnitude compared with those present in the welded built-up sections of similar dimensions. The maximum magnitude reaches 60 to in some cases 90 percent of the yield strength and they distribute over the wide portions of the cross section. Due to the presence of large magnitude of compressive residual stresses in the web plates, there are a number of specimens in which the web plates are critical for buckling. During the bending test of full size rolled beams, it was observed that test beams behaved as if they are made of materials of different strength, which was due to the penetration of premature yielding at portions where a large magnitude of residual stress distributes. A good correlation existed between experimentally obtained moment-curvature relationship and that computed including the effect of residual stress. The fact indicates a large reduction of rigidity even at relatively small loading conditions, however, the width thickness ratios of component plates of rolled beams were so small that stability were not lost by the reduction of rigidity due to the premature yielding and as a consequence the moment carrying capacity inevitably exceeded full plastic moment. It was even noted that a beam with buckled web plates prior to the application of external loads stabilized with the increase of bending moment. The fact can be explained by the theoretical analysis of plate buckling.

References

1) F. Nishino and T. Okumura : "Experimental Investigation of Strength of Plate Girders in Shear" Final Report of 8th Congress of IABSE

2) F. Nishino and T. Okumura : "Strength of Large Size Rolled H-Beams" Annual Report of Eng. Research Inst., Faculty of Eng., Univ. of Tokyo, 1970

3 JAPANESE PROVISIONS ON PLATE GIRDER DESIGN

3.1 Steel Railway Bridges

(Excerpted from the "Specifications for Design of Steel Railway Bridges, 1970" Japanese National Railways)

(1) Thickness Requirements for Web Plates with Intermediate Transverse Stiffeners

For web plate having no longitudinal stiffeners.

Grade of Steel	SS 41 SM 41 SMA 41	SM 50	SM 50Y SM 53 SMA 50	Remarks
Minimum Thickness of Web Plate t (cm)	$\frac{D}{155}$	$\frac{D}{130}$	$\frac{D}{125}$	When the computed compressive stress at the edge of the web plate, σ, is much smaller than the allowable flange compressive stress, the value of t may be calculated by $t = 5400/\sqrt{\sigma} \leqq \frac{D}{200}$

D : clean distance between flanges of a plate girder (cm)

For web plate having one longitudinal stiffener.

Grade of Steel	SS 41 SM 41 SMA 41	SM 50	SM 50Y SM 53 SMA 50	Remarks
Minimum** Thickness of Web Plate (cm)	$\frac{D}{250}$	$\frac{D}{250}$	$\frac{D}{250}$	The gage line of longitudinal stiffener shall be about 0.2D from the toe of the compression flange

** Since plate girders in steel railway bridges are likely to vibrate through the passage of trains and are subject to high local bearing stresses combined with bending stresses when the girders directly support slippers on the top of the flanges, the above thickness requirements which may be sufficiently safe against web buckling in bending are adopted.

(2) Thickness Requirements for Web Plates without Intermediate Transverse Stiffeners

	Grade of Steel	SS 41 SM 41 SMA 41	SM 50	SM 50Y SM 53 SMA 50
Minimum Thickness of Web Plate (cm)	For web plate of a member of which flange plate directly supports sleepers and others	$\frac{D}{70}$	$\frac{D}{60}$	$\frac{D}{55}$
	For web plate of a member carrying no loads on the flange plate	$2000/\sqrt{S/A_w} \leqq \frac{D}{110}$ S : shearing force (kg) A_w : gross sectional area of web plate (cm^2)		

(3) Minimum Moment of Inertia of Stiffeners

Minimum Permissible Moment of Inertia (cm^4)	
intermediate transverse stiffener	longitudinal stiffener
$I = \frac{d_s\, t^3\, r}{11}$	$I = 2d_s\, t^3$ $(d_s/D \leqq 2)$

d_s : actual clear distance between stiffeners (cm)

t : thickness of web plate (cm)

$r = 25\left(\frac{D}{2700t\sqrt{\tau}}\right)^2 - 20 \leqq 5$ τ : mean value of shearing stresses of web plate between two adjacent stiffeners (kg/cm^2)

(4) Allowable Unit Stresses in Bending and Shear

	Allowable Unit Stress (kg/cm^2)		
	SS41 SM41 SMA41	SM 50	SM 50Y SM53 SMA50
Bending			
(1) Tension on extreme fiber(net section)	1,400	1,900	2,100
(2) Compression on extreme fiber (gross section)	1250 for $0<F\frac{\ell}{b}\leqq 28$ $1250-8.0(F\frac{\ell}{b}-28)$ for $28<F\frac{\ell}{b}\leqq 130$ $7{,}400{,}000(b/F\ell)^2$ for $130<F\frac{\ell}{b}$	1700 for $0<F\frac{\ell}{b}\leqq 24$ $1\,700-12.5(F\frac{\ell}{b}-24)$ for $24<F\frac{\ell}{b}\leqq 115$ $7{,}400{,}000(b/F\ell)^2$ for $115<F\frac{\ell}{b}$	1900 for $0<F\frac{\ell}{b}\leqq 22$ $1900-14.8(F\frac{\ell}{b}-22)$ for $22<F\frac{\ell}{b}\leqq 105$ $7{,}400{,}000(b/F\ell)^2$ for $105<F\frac{\ell}{b}$
	ℓ : unsupported length of the compression flange (cm) b : flange width (cm) $F=\sqrt{12+2\beta/\alpha}$ α = flange thickness/web thickness β = D/b		
Shear			
Web of plate girder	800	1,100	1,200

3.2 Steel Highway Bridges

(Excerpted from the "Specifications for Welded Steel Highway Bridges, 1964" Japan Road Association)

(1) Thickness Requirements for Web Plates with Intermediate Transverse Stiffeners

For web plate having no longitudinal stiffeners

Grade of Steel	SS 41	SM 50	SM 50Y SM 53	SM 58
Minimum thickness of web plate (mm)	$\frac{b}{160}$	$\frac{b}{136}$	$\frac{b}{128}$	$\frac{b}{112}$

b : clean distance between flanges of a girder

For web plate having one longitudinal stiffener.

	Portion	Grade of Steel				Remarks
		SS 41	SM 50	SM 50Y SM 53	SM 58	
Minimum Thickness of Web Plate (mm)	b_1	$\frac{b_1}{52}$	$\frac{b_1}{44}$	$\frac{b_1}{41}$	$\frac{b_1}{37}$	When the computed stresses in the portions b_1 and/or b_2 are far small as compared with the allowable stress, the values in the corresponding denominator may be multiplied by $\sqrt{\text{allowable stress}/\text{computed stress}}$
	b_2	$\frac{b_2}{95}$	$\frac{b_2}{81}$	$\frac{b_2}{76}$	$\frac{b_2}{67}$	
	b_3	$\frac{b_3}{207}$	$\frac{b_3}{176}$	$\frac{b_3}{166}$	$\frac{b_3}{146}$	
	b	$\frac{b}{259}$	$\frac{b}{220}$	$\frac{b}{207}$	$\frac{b}{183}$	

The gage line of longitudinal stiffener shall be about 0.2b from the toe of the compression flange.

For web plate having two longitudinal stiffeners.

	Portion	Grade of Steel				Remarks
		SS 41	SM 50	SM 50Y SM 53	SM 58	
Minimum Thickness of Web Plate (mm)	b_1	$\frac{b_1}{49}$	$\frac{b_1}{42}$	$\frac{b_1}{39}$	$\frac{b_1}{35}$	When the computed stresses in the portions b_1, b_2 and/or b_3 are far small as compared with the allowable stress, the values in the corresponding denominator may be multiplied by $\sqrt{\text{allowable stress}/\text{computed stress}}$
	b_2	$\frac{b_2}{55}$	$\frac{b_2}{47}$	$\frac{b_2}{44}$	$\frac{b_2}{39}$	
	b_3	$\frac{b_3}{98}$	$\frac{b_3}{83}$	$\frac{b_3}{78}$	$\frac{b_3}{69}$	
	b_4	$\frac{b_4}{202}$	$\frac{b_4}{172}$	$\frac{b_4}{162}$	$\frac{b_4}{143}$	
	b	$\frac{b}{306}$	$\frac{b}{260}$	$\frac{b}{245}$	$\frac{b}{216}$	

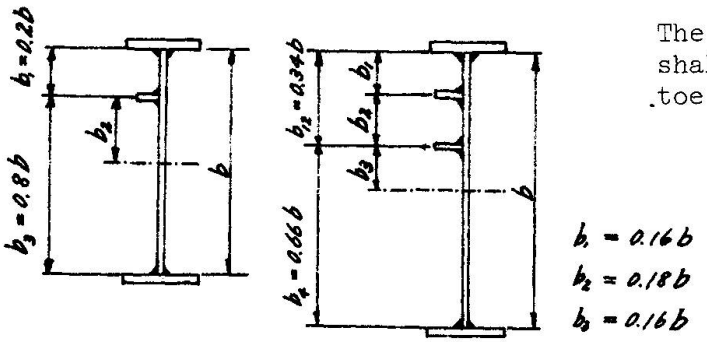

The gage lines of longitudinal stiffeners shall be about 0.16b and 0.34b from the toe of the compression flange.

(2) Thickness Requirements for Web Plates without Intermediate Transverse Stiffeners

Grade of Steel	SS 41	SS 50	SM 50
Minimum thickness of web plate (mm)	$\frac{b}{60}$	$\frac{b}{60}$	$\frac{b}{55}$

(3) Minimum Moment of Inertia of Stiffeners

Minimum permissible moment of inertia (cm^4)	
intermediate transverse stiffener	longitudinal stiffener
$I = \frac{d_o t^3 J}{11}$	$I = \ell t^3 (2.4 \frac{d^2}{\ell^2} - 0.13)$

, where d_o : actual clear distance between stiffeners (cm)

t : thickness of web plate (cm)

$J = 25\left(\frac{\ell}{d}\right)^2 - 20 \geqq 50, \qquad d = \frac{2800\ t}{\sqrt{S/A_{wg}}}$

ℓ : unsupported depth of web plate between flanges (cm)

S : shearing force applied to web plate (kg)

A_{wg} : gross sectional area of web plate (cm^2)

(4) Allowable Unit Stresses in Bending and Shear

Grade of Steel	Allowable Unit Stress (kg/cm^2)			
	SS 41	SS 50	SM 50Y SM 53	SM 58
Bending				
(1) Tension on extreme fiber(net section)	1,400	1,700	2,100	2,600
(2) Compression on extreme fiber(gross section)				
a) when compression flange is unsupported	$1{,}300 - 0.6(\ell/b)^2$ $\ell/b \leqq 30$	$1{,}600 - 0.9(\ell/b)^2$ $\ell/b \leqq 30$	$2{,}000 - 1.4(\ell/b)^2$ $\ell/b \leqq 27$	$2{,}400 - 2.0(\ell/b)^2$ $\ell/b \leqq 25$
	ℓ = unsupported length of the compression flange (cm) b = flange width (cm)			
b) when compression flange is supported laterally its full length by enbedment in concrete	1,300	1,600	2,000	2,400
Shear				
web of plate girder	800	1,000	1,200	1,500

3.3 Plate Girders in Buildings

(Excerpted from the "Specifications for the Design of Steel Structures, 1970" Architectural Institute of Japan)

(1) Check of Web Plate against Plate Buckling

(i) The check of web plate against plate buckling may be omitted provided that

$$\frac{d}{t} \leqq \frac{110}{F} \qquad (1)$$

is satisfied, where

d : clean distance between flanges of a plate girder (cm)

t : thickness of web plate (cm)

F : specified minimum yield point of the grade of steel being used (t/cm^2)

(ii) For the check of web plate against plate buckling, the web plate is sub-divided into rectangular panels of length a and depth d' as shown in Fig. 1. In case two longitudinal stiffeners are used, they must be so placed that the depths of the two subpanels near the compression flange are equal to each other (see Fig. 1).

(iii) The stress caused by external loads in the web plate panel under consideration must satisfy the following inequation:

$$\left(\frac{\sigma}{\sigma_o}\right)^2 + \left(\frac{\tau}{\tau_o}\right)^2 \leqq 1 \qquad (2) \qquad \text{, where}$$

σ : maximum compressive stress at the edge of the web plate panel (t/cm^2)
τ : average shearing stress at the web plate (t/cm^2)
σ_o : allowable plate buckling stress in bending (t/cm^2)
τ_o : allowable plate buckling stress in shear (t/cm^2)

(iv) Allowable plate buckling stress in bending δ_o

$$\sigma_o = \frac{1900}{(c_1 \frac{d'}{t})^2} f_t \qquad \text{for} \quad \frac{d'}{t} \geqq \frac{56}{c_1}$$

$$= (1.78 - 0.021\, c_1 \frac{d'}{t}) f_t \leqq f_t \qquad \text{for} \quad \frac{d'}{t} < \frac{56}{c_1} \qquad (3)$$

In case $d/t \leqq 210/\sqrt{F}$, the value of σ_o may be taken as f_t.

Notations : $c_1 = F/k_1$

$k_1 = (1 + \frac{\alpha}{6})(\alpha^3 + 3\alpha^2 + 4)$

$\alpha = 1 - \sigma_{min}/\sigma$: coefficient of compressive stress distribution(see Fig. 2)

f_t : allowable tensile stress (t/cm^2)

(v) Allowable plate buckling stress in shear.

$$\tau_o = \frac{3{,}300}{(c_2 \frac{d}{t})} \frac{f_t}{\sqrt{3}} \qquad \text{for} \quad \frac{d}{t} \geqq \frac{74}{c_2}$$

$$= (1.74 - 0.0154\, c_2 \frac{d}{t}) \frac{f_t}{\sqrt{3}} \leqq \frac{f_t}{\sqrt{3}} \qquad \text{for} \quad \frac{d}{t} < \frac{74}{c_2} \qquad (4)$$

Notations : $c_2 = F/k_2$

In case no longitudinal stiffener is used,

$$k_2 = 4.00 + \frac{5.34}{\beta^2} \quad \text{for} \quad \beta < 1.0 \qquad k_2 = 5.34 + \frac{4.00}{\beta^2} \quad \text{for} \quad \beta \geqq 1.0 \qquad (5)$$

In case one or two longitudinal stiffener is used,

$$k_2 = 4.00 + \frac{5.34}{\beta^2} + \frac{(n+1)^2 \eta}{\beta} \sqrt{\frac{8\mu}{3\beta}} \qquad \text{for } \beta < 1.0$$

$$k_2 = 5.34 + \frac{4.00}{\beta^2} + \frac{(n+1)^2 \eta}{\beta} \sqrt{\frac{8\mu}{3\beta}} \qquad \text{for } \beta \geqq 1.0 \qquad (6)$$

$\beta = a/d$ (see Fig. 2)

n = number of longitudinal stiffeners (i.e., n=1 or 2)

$\eta = \frac{d'}{d}$

$\mu = 10.9\, I_L/dt^3$

I_L : moment of inertia of longitudinal stiffener(s) (cm^4)

(2) Minimum Moment of Inertia of Intermediate Transverse Stiffeners

In case no longitudinal stiffener is used,

$$I_o = 1.1\ dt^3\left(\frac{1}{\beta^2} - 0.5\right) \qquad \text{for } \beta < 1.0$$

$$= 0.55\ dt^3 \qquad \text{for } \beta \geq 1.0 \qquad (7)$$

, where I_o denotes the required minimum moment of inertia of intermediate stiffeners.

In case one or two longitudinal stiffener is used,

$$I_o = 1.1\ dt^3\left(\frac{1}{\beta'^2} - 0.5\right) \qquad \text{for } \beta' < 1.0$$

$$= 0.55\ dt^3 \qquad \text{for } \beta' \geq 1.0 \qquad (8)$$

, where β' represents an aspect ratio a/d for which the value of τ_o computed by the use of Eq.(6) with the actual value of β is equal to that computed by the use of Eq.(5) with $\beta=\beta'$.

(3) Minimum Radius of Gyration of Longitudinal Stiffeners

$$\frac{i}{t} = C_m\{135(0.5 - \eta)^2 + 3\}\beta^{2/3}$$

$$C_m = 0.7 + \frac{1}{200(n+1)}\ \frac{i}{t}\ \frac{1}{\delta}$$

, where $0.2 \leqq \eta = \frac{d'}{d} \leqq 0.5$ for $n = 1$

$0.15 \leqq \eta = \frac{d'}{d} \leqq 0.3$ for $n = 2$

Notations :

$$\delta = \frac{A_s}{dt}$$

A_s : cross-sectional area of longitudinal stiffeners (cm^2)

---

* The minimum yield points for the six grades of steel are as follows:

Grade of Steel	SS 41	SS 50	SM 50	SM 50Y	SM 53	SM 58
Minimum Yield Point(kg/cm^2)	2,300	2,800	3,200	3,600	3,600	4,600

3.4 Ship Structures

The shape of girders used in ship structures are more complex compared to bridge or building structures. Namely, the girders are of variable cross sections and the height of webs become large at the corner connections. Furthermore, the girders have many holes in the web plate for man holes, piping holes and slots for longitudinal members.

The web height-thickness ratios of bottom transverses in wing tank are shown in Fig. 3. Fig. 4 shows the detailed dimensions of a bottom transverse in wing tank for different size (dead weight tonnages) of ships.

According to the increasing size of ships, the web height increases, on the other hand, the web thickness have hardly increased. This results the ratios h/t_w become high for huge tankers.

Thickness requirements of Nippon Kaiji Kyokai Rule (1970) for web plate of bottom transverses are as follows,

$$t_w = C_{do} + 3.5 \leq t_{min} \qquad (10)$$

where t_w : required web thickness (mm)

d_o : web height (m)

$C=C_1$: for web plate without horizontal stiffeners

$C=C_2$: for the panels between a horizontal stiffener and the bottom plate.

$C=C_3$: for the panels between horizontal stiffeners or between a horizontal stiffener and the flange plate

C_1, C_2 and C_3 are given in the table below, and when there are slots or holes, the modified C value should be used.

S*/do	≤0.2	0.4	0.6	0.8	1.0	1.5	2.0	2.5≤
C_1	2.6	4.5	5.6	6.4	7.1	7.8	8.2	8.4
C_2	2.1	3.7	4.9	5.8	6.6	7.4	7.8	8.0
C_3	3.7	6.7	8.6	9.6	10.3	10.4	10.4	10.4

* S : space of vertical stiffeners

Minimum thickness t_{min} in eq. (10) is specified in the table below.

Length of Ship (m)	105	105 – 120	120 – 135	135 – 150	150 – 165	165 – 180	180 – 195	195 – 225	225 – 275	275 –
t_{min} (mm)	8.0	8.5	9.0	9.5	10.0	10.5	11.0	11.5	12.0	12.5

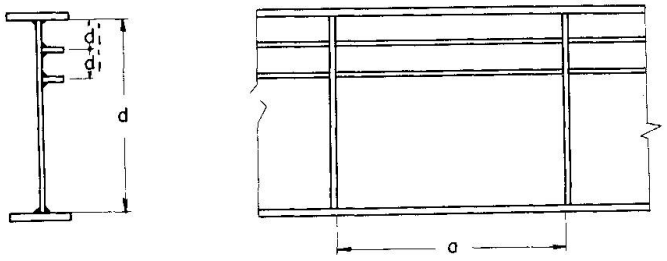

Fig. 1

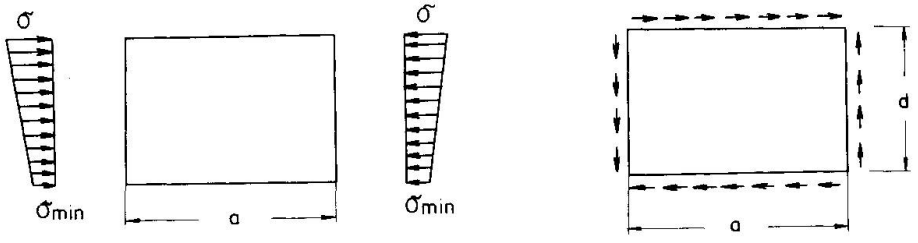

Fig. 2

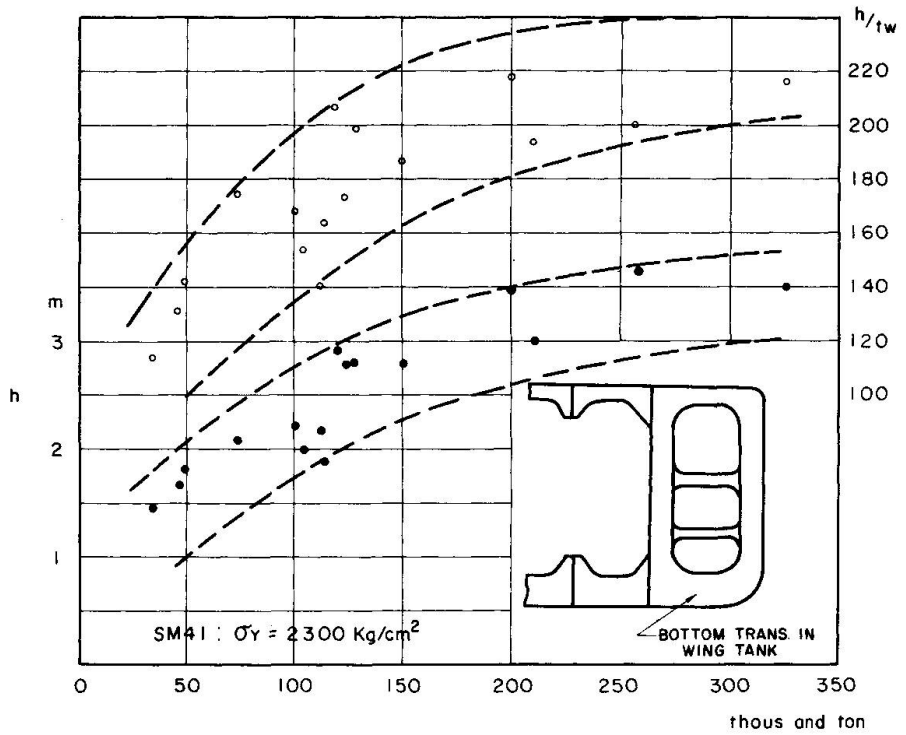

Fig. 3 Web Heights (or Web Height – Thickness Ratio) and Dead Weight Tonnages of Tankers for Bottom Transverses in Wing Tanks.

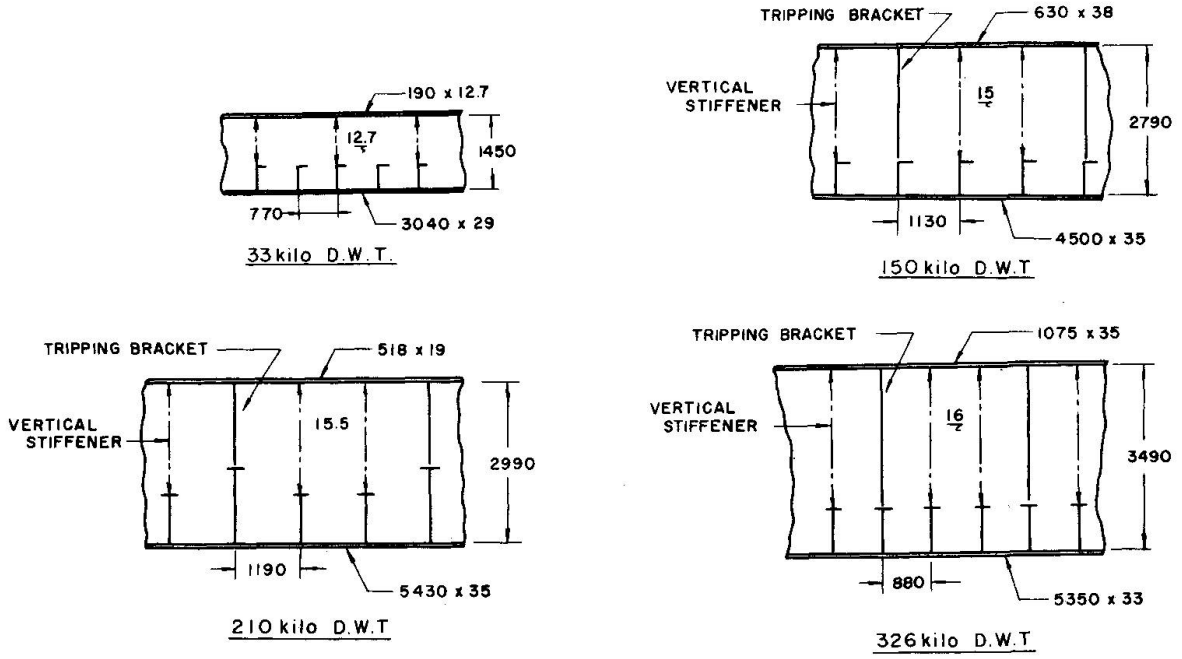

Fig. 4 Detailed Dimensions of Bottom Transverses in Wing Tanks for different Dead Weight Tonnages of Tankers.